ARTICLE

Acridinium salts as photoredox organocatalysts for photomediated cationic RAFT and DT polymerizations of vinyl ethers†

Received 00th January 20xx,
Accepted 00th January 20xx

DOI: 10.1039/x0xx00000x

Marina Matsuda,[a] Mineto Uchiyama,[a] Yuki Itabashi,[b] Kei Ohkubo[*b,c] and Masami Kamigaito[*a]

A series of acridinium salts with high excited-state oxidative power are employed as photoredox organocatalysts in conjunction with various thioesters, such as trithiocarbonate, dithiocarbamate, and xanthate, and thioacetals for photomediated cationic reversible addition-fragmentation chain-transfer (RAFT) and degenerative chain-transfer (DT) polymerizations of vinyl ethers under visible light. A combination of acridinium salts and trithiocarbonate or thioacetal induces relatively fast and controlled cationic polymerization of various alkyl vinyl ethers under blue, green, and white LEDs, where the photoexcited acridinium salts generate cationic species from the sulfur compounds via the mesolytic cleavage of carbon-sulfur bonds through the formation of radical cations. An acridinium salt with a higher excited-state oxidative power induces faster cationic polymerization. Temporal control of the polymerization is achievable by switching the light on and off, although the polymerization in the dark is not completely halted. The controlled nature of the polymerization further enables the synthesis of block copolymers of alkyl vinyl ethers via sequential monomer addition.

Introduction

Photoredox catalysts are increasingly attracting much attention because they can mediate new efficient organic reactions under mild conditions with light irradiation.[1–6] In general, excited photoredox catalysts can activate substrates via single electron transfer to generate radical cations or anions as reactive intermediates and to efficiently induce selective reactions, which are difficult to attain under thermal conditions.

In addition to organic reactions, photoredox catalysts can also mediate polymerizations under light-irradiated mild conditions to enable precision synthesis of tailor-made macromolecules with precise structural design,[7–10] as summarized in the review by Yagci, who has greatly contributed to the developments of polymer chemistry based on photomediated polymerizations and polymer syntheses.[9,11,12] In particular, recent advances in various metal or organic photoredox catalysts have contributed to great developments in controlled/living or reversible deactivation radical polymerization (RDRP), such as atom transfer radical polymerization (ATRP)[13–19] and reversible addition-fragmentation chain transfer (RAFT)[20–25] polymerization, because they enable reversible formation of radical species from dormant species with covalent carbon-halogen and carbon-sulfur bonds even at room temperature, where thermal-induced side reactions are suppressed and fine control is thus enhanced. In most cases, these photoredox catalysts are excited by visible or ultraviolet (UV) light to obtain a potential high enough to reduce the stable dormant species to radical anions and to generate the propagating radical species via mesolytic cleavage of the covalent bonds.

Recently, photoredox catalysts have also been used for harnessing photocontrolled options for cationic RAFT and degenerative chain transfer (DT) polymerizations, in which covalent carbon-sulfur and carbon-oxygen bonds work as dormant species.[26–32] The first photoredox catalyst used in cationic DT polymerization was a pyrylium salt, which was used by You, Nicewicz and Perkowski for *p*-methoxystyrene (pMOS) in the presence of methanol as a precursor of a reversible chain-transfer agent under blue LED irradiation.[33] Later, Fors and coworkers employed not only a series of pyrylium salts but also iridium salts for vinyl ethers in conjunction with thioesters and thioacetals as the dormant species to attain photoresponsive control of cationic RAFT and DT polymerizations and clarified the polymerization mechanism.[34–38] More recently, Liao et al. developed novel bisphosphonium salts as more active catalysts for cationic RAFT polymerization.[39] All these photoredox catalysts have relatively high oxidative power in the excited states and thus

[a] *Department of Molecular and Macromolecular Chemistry, Graduate School of Engineering, Nagoya University, Furo-cho, Chikusa-ku, Nagoya 464-8603, Japan, E-mail: kamigait@chembio.nagoya-u.ac.jp.*
[b] *Institute for Open and Transdisciplinary Research Initiatives, Osaka University, Suita, Osaka 565-0871, Japan, E-mail: ohkubo@irdd.osaka-u.ac.jp*
[c] *Institute for Advanced Co-Creation Studies, Osaka University, Suita, Osaka 565-0871, Japan.*

Electronic Supplementary Information (ESI) available: [details of any supplementary information available should be included here]. See DOI: 10.1039/x0xx00000x

oxidize the dormant species to radical cations under light to generate the propagating cationic species via mesolytic cleavage of the covalent bonds.

Acridinium salts, which were disclosed by Fukuzumi, Ohkubo and coworkers and have been further developed by Nicewicz and coworkers, are known as photoredox catalysts with a highly positive excited-state reduction potential (E^*_{red} = up to 2.06 V vs. SCE), i.e., a high excited-state oxidative power, and a long lifetime in the excited states with intramolecular charge separation.[40–44] A series of acridinium salts with various substituents at different positions have been synthesized to tune the photoredox catalytic abilities and have been used for various organic reactions. However, there have been no successful results on their use for cationic RAFT and DT polymerizations except for preliminary negative results with no polymerizations.[36] In addition to their use for cationic polymerization, there is one report on the photoradical polymerization of (meth)acrylates with acridinium salts as photosensitizers.[45] Furthermore, acridinium salt was also tried in a photoinduced ring-opening metathesis polymerization, though it showed no activity.[46] This is in contrast to acridine, which has been widely used for photo- or photoredox catalysts for cationic and radical polymerizations.[47–50]

In this study, we investigated cationic RAFT and DT polymerizations of various vinyl ethers, such as isobutyl (IBVE), ethyl (EVE), isopropyl (IPVE) and 2-chloroethyl vinyl ether (CEVE), using a series of acridinium salts (**A1–A6**) in conjunction with various sulfur compounds, including trithiocarbonate (**C1**), dithiocarbamate (**C2** and **C3**), xanthate (**C4**), and thioacetal (**C5**), under visible light irradiation with blue, green, and white LEDs (Scheme 1). In addition, temporal control with light and block copolymer synthesis were examined.

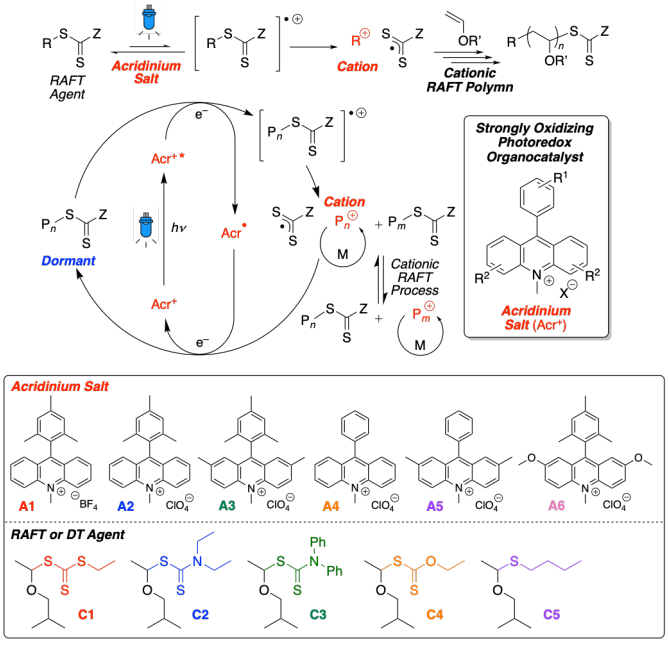

Scheme 1. Photomediated cationic RAFT and DT polymerization using acridinium salts.

Results and discussion

Various acridinium salts (A1–A6) and trithiocarbonate (C1) for IBVE polymerization under blue LED irradiation

The cationic polymerization of IBVE was examined using a series of acridinium salts (**A1–A6**) with various substituents and different counteranions (BF_4^- and ClO_4^-) in conjunction with trithiocarbonate (**C1**) under blue LED (470 nm, 70 mW) irradiation in CH_2Cl_2 at –40 °C (Fig. 1).[51] No polymerization occurred only with acridinium salts such as **A1** without trithiocarbonate even under light irradiation. In addition, in the dark with **C1**, the acridinium salts did not induce any polymerization. However, under a blue LED and in the presence of **C1**, all acridinium salts led to relatively fast consumption of IBVE. In particular, **A4**, which possesses the highest excited-state reduction potential, led to the fastest reaction to complete the monomer consumption within 3 min. The order of overall polymerization rates using acridinium salts with ClO_4^- decreased in the following order: **A4** > **A5** > **A3** > **A2** > **A6**. The reactivity depends on the oxidative abilities, i.e., one-electron reduction potentials: 2.25 V vs. SCE for **A4**, 2.17 V for **A5** at the excited states[52] and 2.06 V for **A3**, **A2** and **A6** in the electron transfer state.[53] The high reactivity of **A3** is derived from the strong catalyst-recovery ability due to more negative one-electron oxidation potential of the electron-transfer state of **A3** (E_{ox} = –0.67 V) than that of **A2** (–0.57 V).[50] The lower catalytic reactivity of **A6** comes from the smaller quantum yield of electron-transfer state to be Φ = 0.5 rather than those of **A2** and **A3** (Φ = 0.98).[40,53,54] The counteranion also had effects on the polymerization rates, where the reaction with **A1** possessing BF_4^- was slower than **A2** with ClO_4^-, although their redox potentials were almost the same.

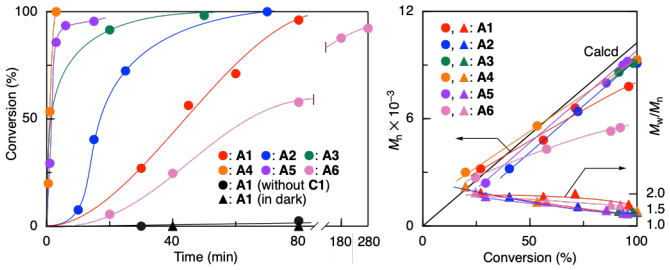

Fig. 1. Photomediated cationic RAFT polymerization of IBVE using various acridinium salts (**A1–A6**) and trithiocarbonate (**C1**) in CH_2Cl_2 at –40 °C under irradiation of blue LED: $[M]_0/[C1]_0/[acridinium\ salt]_0$ = 500/5.0 or 0/0.50 or 0.20 mM.

The size-exclusion chromatography (SEC) curves of all the obtained polymers were unimodal and became narrower as the polymerization proceeded. The number-average molecular weights (M_n) increased in direct proportion to monomer conversion and agreed well with the calculated values assuming that one trithiocarbonate molecule (**C1**) generates one polymer chain.

The ^{1}H NMR spectrum of the polymers obtained with a combination of **C1** and **A2** showed the presence of a trithiocarbonate group at the ω-end and a methyl group at the α-end (Fig. S1 in the electronic supplementary information (ESI)). The M_n value (M_n(NMR) =7700), which was calculated

from the peak intensity ratio of the terminal methine proton (*b'*) at the ω-end and the main-chain methine (*b*) and methylene (*c*) protons attached to the ether oxygen in the repeating monomer units, was close to that measured by SEC (M_n(SEC) = 7300), suggesting that almost all the polymer chains were generated from **C1**.

These results indicate that three components consisting of acridinium salt, trithiocarbonate, and light are necessary to induce the cationic polymerization of IBVE. The acridinium salts thus selectively cleave the carbon-sulfur bond of trithiocarbonate under blue LED to generate the cationic species and induce the cationic RAFT polymerization of IBVE. In this case, trithiocarbonate plays dual roles as an initiator, which generates the initiating cationic species via mesolytic cleavage of the C–S bond by the excited acridinium salts, and as a chain-transfer agent, which undergoes heterolytic cleavage of the C–S bond attacked by the propagating cationic species, and thereby controls the molecular weights and chain-end groups of the resulting polymers.

Various sulfur compounds (C1–C5) and A1 for IBVE polymerization under blue LED irradiation

To clarify the effective compounds working as both initiators and RAFT agents in the photomediated cationic polymerization, various sulfur compounds (**C1**–**C5**), which have been employed for cationic RAFT and DT polymerizations of vinyl ethers initiated with strong protonic acids,[26–31] were used in conjunction with the acridinium salt with BF_4^- (**A1**) in CH_2Cl_2 at –40 °C under blue LED for IBVE polymerization (Fig. 2).

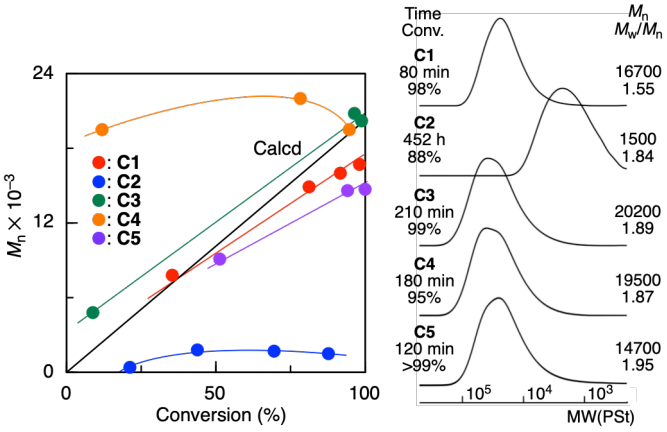

Fig. 2. Photomediated cationic RAFT polymerization of IBVE using various RAFT or DT agents and acridinium salt (**A1**) in CH_2Cl_2 at –40 °C under irradiation of blue LED: $[M]_0/[\text{RAFT or DT agent}]_0/[\mathbf{A1}]_0$ = 1000 or 500/5.0 or 2.5/0.50 mM.

In all cases, IBVE was quantitatively consumed. However, the molecular weights depended on the structures of the leaving groups of the sulfur compounds. As with trithiocarbonate (**C1**), a linear molecular weight increase was observed with *N*,*N*-diphenyldithiocarbamate (**C3**) and thioacetal (**C5**), which both have relatively high chain-transfer constants in the cationic RAFT polymerization initiated with triflic acid, although the molecular weight distributions (MWDs) were slightly broader than those with **C1**. In addition, xanthate (**C4**) resulted in M_n values that were higher than the calculated values in the initial and middle stages of the polymerizations and became close to the calculated values at the later stage. This is due to the lower chain-transfer constant of **C4** than that of **C1**, as reported in the cationic RAFT polymerization with TfOH.[27–29,31] In contrast, *N*,*N*-diethyldithiocarbamate (**C2**), which is a highly efficient RAFT agent in the presence of TfOH,[29,31] only gave polymers with low molecular weights (M_n < 2000) throughout the reactions and thus was not effective for controlling the cationic polymerization with acridinium salts. This could be attributed to the *N*,*N*-diethyl group in the dithiocarbamate being oxidized by the excited acridinium salt with a high oxidative power and decomposed. Therefore, trithiocarbonate (**C1**) proved most suitable for acridinium-mediated cationic RAFT polymerization.

Temporal control of polymerization

The temporal control of the polymerization by intermittent light exposure was examined by switching the blue LED on and off using **C1** and **A1** for IBVE polymerization in CH_2Cl_2 at –40 °C (Fig. 3). When the monomer conversion reached 16% after 10 min of irradiation, the light was turned off for 25 min. After switching off the light, the polymerization rate was significantly decreased, although the polymerization was not completely stopped in the dark. However, after the light was turned on again, the smooth consumption of monomer started again and reached 42% in the additional 10 min exposure to light. During additional two-cycle procedures consisting of switching the light off and on, a similarly decreased polymerization rate in the dark and fast polymerization under blue LED were further observed. The M_n values increased in direct proportion to monomer conversion throughout these processes. In addition, the MWDs became narrower as the molecular weights increased. These results indicate that the formation of the cationic propagating species was triggered by light via mesolytic cleavage of the thioester bond at the dormant polymer terminal.

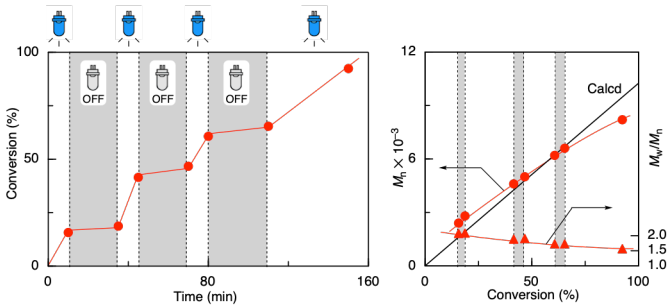

Fig. 3. Temporal control of photomediated cationic RAFT polymerization of IBVE with **C1**/**A1** in CH_2Cl_2 at –40 °C by switching blue LED on and off: $[M]_0/[\mathbf{C1}]_0/[\mathbf{A1}]_0$ = 500/5.0/0.20 mM.

However, immediate capping of the formed cation in the dark was not attained, most likely due to slow reduction of the trithiocarbonyl radical or its dimer into the trithiocarbonate anion by the reduced form of the acridinium salt, i.e., acridine radical. A similar imperfect temporal control was also reported for pyrylium salts, whereas iridium salts with a higher stability and more reducing ground state potential enabled complete

halt of the polymerizations in the dark.[33–36] A complete halt using iridium salt was also reported for photomediated cationic polymerization via mesolytic cleavage of alkoxyamine.[55]

Effects of solvents

To examine the effects of solvent polarity on the cationic polymerization, *n*-hexane was used as a cosolvent for CH_2Cl_2 in the cationic polymerization of IBVE with **C1** and **A2** at –40 °C (Fig. 4). In general, the addition of a nonpolar solvent such as *n*-hexane retards cationic polymerization due to the low dielectric constant. Contrary to our expectation, the polymerization in a 1/1 (v/v) mixture of *n*-hexane and CH_2Cl_2 became faster than that in CH_2Cl_2 and completed in 7 min. The obtained polymer had controlled molecular weights and narrower MWDs (M_w/M_n = 1.34). The fast polymerization could be attributed to the nonpolar solvent contributing to the charge separation of the excited acridinium salt, resulting in high activity.[56,57] Under the condition with a much higher *n*-hexane content (*n*-hexane/CH_2Cl_2 = 4/1), the concentration of acridinium salt had to be lowered from 0.50 to 0.20 mM due to the insolubility of **A2** in *n*-hexane. Although the polymerization rate was decreased by lowering the concentration of **A2**, the polymerization was nearly completed in 80 min, where the rate was almost the same as that in CH_2Cl_2 with 0.50 mM **A2**, resulting in the narrowest MWD (M_w/M_n = 1.24).[58]

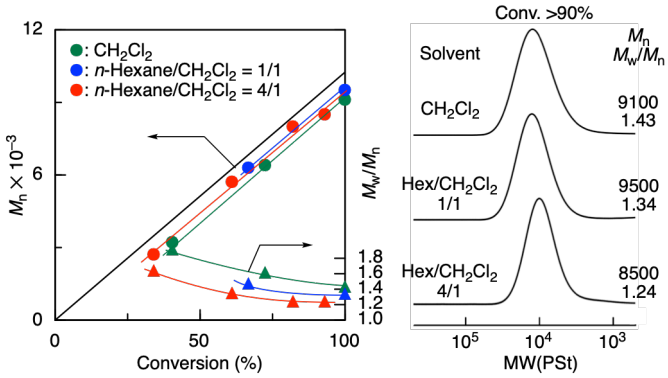

Fig. 4. Solvent effects on photomediated cationic RAFT polymerization of IBVE with **C1**/**A2** at –40 °C under irradiation of blue LED: $[M]_0/[\mathbf{C1}]_0/[\mathbf{A2}]_0$ = 500/5.0/0.50 or 0.20 mM.

In addition, a similar solvent effect was observed for cationic DT polymerization using thioacetal (**C5**) in conjunction with **A2** in the mixed solvent (*n*-hexane/CH_2Cl_2 = 4/1) at –40 °C under blue LED, where a similarly controlled molecular weight and narrow MWD were attained (M_n = 11100, M_w/M_n = 1.22) (Fig. S3 in ESI†). The MALDI-TOF-MS spectrum of the obtained polymers showed the presence of thioacetal at the chain end of the obtained polymers (Fig. S4 in ESI†). These results indicate that thioacetal is also effective for DT polymerization in the presence of **A2** under appropriate conditions with visible light irradiation.

Polymers with high and controlled molecular weights

Since suitable conditions were found to control the cationic polymerization of IBVE with acridinium salts, the synthesis of high-molecular-weight polymers was investigated by changing the feed ratio of monomer to trithiocarbonate (**C1**) in the presence of **A2** under blue LED in mixed solvents of *n*-hexane and CH_2Cl_2 (4/1 or 3/1) at –40 °C (Fig. 5). Irrespective of the feed ratios, polymerization efficiently occurred to give polymers with relatively narrow MWDs (M_w/M_n ~ 1.2) in all cases. The M_n increased in direct proportion to the feed ratio of IBVE to **C1** and finally reached 40000 at the 500/1 feed ratio. Thus, the initiating system consisting of acridinium salt and trithiocarbonate proved effective for controlling the cationic polymerization of IBVE under blue LED.

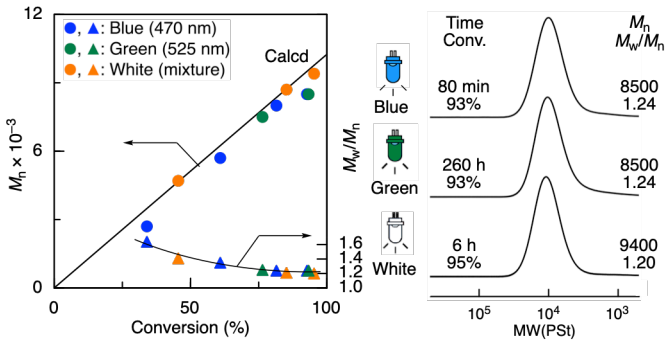

Fig. 6. Photomediated cationic RAFT polymerization of IBVE with **C1**/**A2** in *n*-hexane/CH_2Cl_2 (4/1) at –40 (blue and white LED) or –20 (green LED) °C under irradiation of blue (470 nm), green (525 nm) and white LED (mixture): $[M]_0/[\mathbf{C1}]_0/[\mathbf{A2}]_0$ = 500/5.0/0.20 mM.

Effects of light wavelength

Since acridinium salts have strong absorptions in visible light regions,[56] LEDs with different colors or wavelengths could work for the excitation of acridinium salts to mediate cationic polymerization. Upon irradiation of green (λ_{max} = 525 nm, 20 mW) and white (470 nm, 50 mW/525 nm, 45 mW/630 nm, 40 mW) LEDs, polymerizations with the **C1**/**A2** initiating system also proceeded, although polymerization under a green LED was very slow even at –20 °C. However, all the obtained

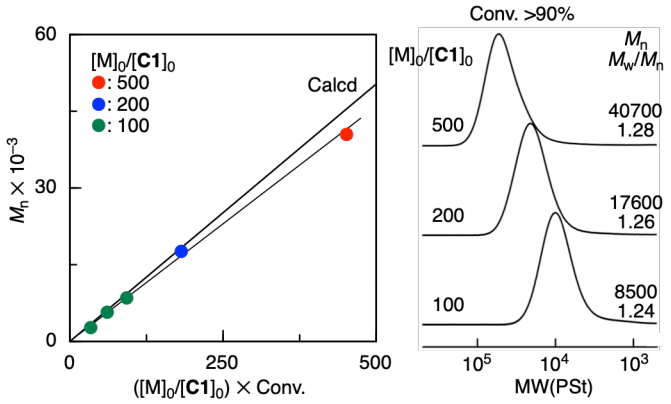

Fig. 5. Synthesis of polymers with high and controlled molecular weights in photomediated cationic RAFT polymerization of IBVE with **C1**/**A2** in *n*-hexane/CH_2Cl_2 (4/1 or 3/1) at –40 °C under irradiation of blue LED: $[M]_0/[\mathbf{C1}]_0/[\mathbf{A2}]_0$ = 1000 or 500/5.0, 2.5, or 2.0/0.20 mM.

polymers possessed controlled molecular weights and narrow MWDs (M_w/M_n ~ 1.2) (Fig. 6). These results indicate that acridinium salts can be used for cationic RAFT polymerization under irradiation with visible light of various wavelengths.

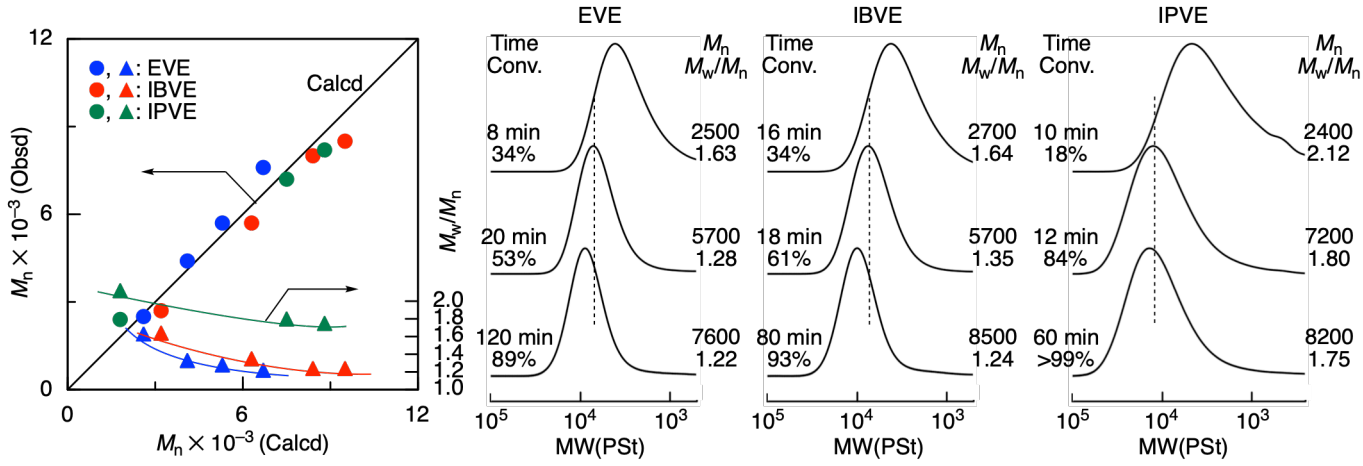

Fig. 7. Photomediated cationic RAFT polymerization of EVE, IBVE and IPVE with **C1**/**A2** in *n*-hexane/CH_2Cl_2 (4/1) at –40 °C under irradiation of blue LED: $[M]_0/[\mathbf{C1}]_0/[\mathbf{A2}]_0$ = 500/5.0/0.20 mM.

Cationic polymerization of various monomers

To observe the versatility of the acridinium salts for various monomers, other alkyl vinyl ethers, such as EVE and IPVE, were polymerized with the same initiating system (**C1**/**A2**) in *n*-hexane/CH_2Cl_2 (4/1) at –40 °C under a blue LED (Fig. 7). Both monomers were polymerized efficiently. In particular, IPVE, which is a secondary alkyl vinyl ether and is more reactive than a primary vinyl ether, was polymerized faster than IBVE and EVE. The M_n values of all the obtained polymers increased in direct proportion to monomer conversion and agreed well with the calculated values. The MWDs of poly(EVE) were similarly narrow (M_w/M_n ~ 1.2), whereas those of poly(IPVE) were slightly broader due to the fast propagation of IPVE. In the cationic RAFT polymerization of IPVE, the addition fragmentation process could be slow because the secondary alkyl group increases the steric hindrance around the terminal and retards the addition fragmentation process.[30] The ^{1}H NMR spectra of all the obtained polymers showed that the polymers possessed trithiocarbonate termini almost quantitatively (Fig. S5 in ESI†). Thus, various alkyl vinyl ethers can be polymerized in a controlled manner with acridinium salt under visible light irradiation.

In contrast, the polymerization of CEVE with **C1**/**A2** in CH_2Cl_2 at –40 °C was very slow (97% in 72 h) and not controlled, resulting in polymers with tailings in low molecular weight regions of the SEC curves (M_n = 1800. M_w/M_n = 2.29). This was attributed to the high excited-state oxidative power of the acridinium salt, which could oxidize the pendant chloroethyl substituent. The polymerization of *p*-methoxystyrene (pMOS) was also examined using **C1**/**A1** in CH_2Cl_2 at –40 °C. Although the monomer was consumed (32% in 20 h), the products were only low molecular weight compounds, suggesting that pMOS itself underwent oxidation by the exited acridinium salt, as reported for visible-light-mediated [4+2] cycloaddition reactions of styrenes with acridinium salts.[59]

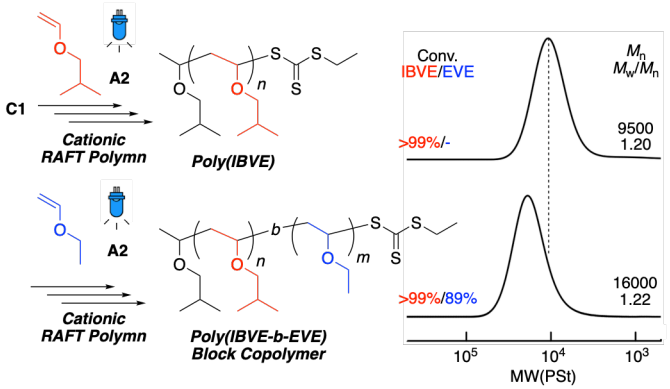

Fig. 8. Photomediated cationic RAFT block polymerization of IBVE and EVE with **C1**/**A2** in *n*-hexane/CH_2Cl_2 (4/1) at –40 °C under irradiation of blue LED: $[IBVE]_0/[EVE]_{add}/[\mathbf{C1}]_0/[\mathbf{A2}]_0$ = 500/500/5.0/0.20 mM.

Block copolymerization

Finally, the versatility of acridinium salts for the polymerizations of alkyl vinyl ethers prompted us to examine block copolymerization of IBVE and EVE (Fig. 8). IBVE was thus first polymerized with the **C1**/**A2** initiating system in *n*-hexane/CH_2Cl_2 (4/1) at –40 °C under a blue LED to result in polymers with a controlled molecular weight and narrow MWD (M_n = 9500, M_w/M_n = 1.20). After IBVE was nearly consumed (Conv. > 99%), an equimolar amount of EVE to that of IBVE was added. The added EVE was smoothly polymerized to result in a shift of the SEC curves of the products to high molecular weights (M_n = 16000, M_w/M_n = 1.22) without any remaining homopolymers of IBVE. ^{1}H NMR analysis also confirmed the formation of block copolymers of IBVE and EVE (Fig. S6 in ESI†).

Conclusions

In conclusion, acridinium salts were effective for photomediated cationic RAFT and DT polymerizations of alkyl vinyl ethers in the presence of thioesters and thioacetals under visible light with a wide range of wavelengths. The obtained polymers possessed controlled molecular weights, narrow molecular weight distributions, and thioester and thioacetal chain-end groups. The versatility and chain-end fidelity enabled the precision synthesis of block copolymers of alkyl vinyl ethers. The polymerization was responsive to photoirradiation, although polymerization could not be completely halted by switching the light off. The high excited-state oxidative power of acridinium salts could contribute to further developments of photocontrolled precision polymerizations.

Experimental section

Materials

Isobutyl vinyl ether (IBVE) (Tokyo Kasei, >95%), isopropyl vinyl ether (IPVE) (Wako, 97%), ethyl vinyl ether (EVE) (Tokyo Kasei, >98%), 2-chloroethyl vinyl ether (Tokyo Kasei, >97%), *p*-methoxystyrene (pMOS) (Tokyo Kasei, >98.0%), and *o*-dichlorobenzene (Wako, 98.0%) were distilled over calcium hydride under reduced or atmospheric pressure. 9-Mesityl-10-methylacridinium tetrafluoroborate (**A1**) (Sigma–Aldrich), 9-mesityl-10-methylacridinium perchlorate (**A2**) (Tokyo Kasei, >98.0%), 9-mesityl-2,7,10-trimethylacridinium perchlorate (**A3**) (Tokyo Kasei, >98.0%), and 10-methyl-9-phenylacridinium perchlorate (**A4**) (Tokyo Kasei, >98.0%) were used as received. All the acridinium salts were handled in a glove box (MBRAUN LABmaster sp) under a moisture- and oxygen-free argon atmosphere (O_2, <1 ppm). *n*-Hexane (KANTO, >96%; H_2O <10 ppm) and CH_2Cl_2 (Kanto, >99.5%, H_2O <20 ppm) were dried and deoxygenated by passage through a Glass Contour Solvent System before use. *S*-1-Isobutoxyethyl *S'*-2-ethyl trithiocarbonate (**C1**),[60] *S*-1-isobutoxyethyl *N*,*N*-diethyl dithiocarbamate (**C2**),[29] *S*-1-isobutoxyethyl *N*,*N*-diphenyl dithiocarbamate (**C3**),[29] *S*-1-isobutoxyethyl *O*-ethyl xanthate (**C4**),[61] and butyl(1-isobutoxyethyl)thioacetal (**C5**)[30] were synthesized according to literature procedures.

Synthesis of 2,7,10-trimethyl-9-phenylacridinium perchlorate (A5)

A 100 mL round-bottomed flask was charged with 4,4'-dimethyldiphenylamine (590 mg, 3.0 mmol, 1.0 equiv.) and *N,N*-dimethylformamide (30 mL) under a N_2 atmosphere. Sodium hydride (60% dispersion in mineral oil, 129 mg, 3.3 mmol, 1.1 equiv.) was added slowly at 0 °C. The mixture was allowed to warm to room temperature and stirred for 1 h. Iodomethane (511 mg, 3.6 mmol, 1.2 equiv.) was added dropwise and then stirred for 3 h. The reaction mixture was quenched with water, and the aqueous layer was extracted with chloroform. The combined organic layers were washed with brine, dried over magnesium sulfate, and filtered. The filtrate was concentrated *in vacuo* to afford a thick oil. The oil was added to a flask with benzoyl chloride (1.3 g, 9.0 mmol) and *o*-dichlorobenzene (20 mL). Trifluoromethanesulfonic acid (45 mg, 0.30 mmol) was added slowly and stirred at 140 °C for 16 h. The reaction mixture was quenched with a saturated solution of sodium bicarbonate, and the aqueous layer was extracted with chloroform. The combined organic layers were stirred with sodium perchlorate for 1 h and filtered. The filtrate was concentrated *in vacuo* to afford a crude mixture. The mixture was separated by silica gel column chromatography (eluent: chloroform/methanol = 20/1 to 10/1) to a yellow crude solid. The crude material was recrystallized with chloroform and hexane to afford 2,7,10-trimethyl-9-phenylacridinium perchlorate as a yellow powder (700 mg, 59% yield). ^{1}H NMR (Fig. S7 in ESI†) (400 MHz, chloroform-*d*) δ 8.60 (d, *J* = 9.2 Hz, 2H), 8.17 (dd, *J* = 9.2, 1.8 Hz, 2H), 7.76-7.70 (m, 3H), 7.63 (s, 2H), 7.46-7.44 (m, 2H), 5.03 (s, 3H), 2.54 (s, 6H). ^{13}C NMR (Fig. S8 in ESI†) (101 MHz, chloroform-*d*) δ 158.7, 141.1, 139.8, 138.4, 133.3, 130.2, 129.6, 129.0, 127.9, 126.4, 118.4, 39.3, 21.5. HRMS (Fig. S9 in ESI†): calcd for $C_{22}H_{20}N^+$, 298.1590; found, 298.1600.

Synthesis of 9-mesityl-2,7-dimethoxy-10-methylacridinium perchlorate (A6)

A 100 mL round-bottomed flask was charged with 4,4'-dimethoxydiphenylamine (688 mg, 3.0 mmol, 1.0 equiv.) and *N,N*-dimethylformamide (30 mL) under a N_2 atmosphere. Sodium hydride (60% dispersion in mineral oil, 130 mg, 3.3 mmol, 1.1 equiv.) was added slowly at 0 °C. The mixture was allowed to warm to room temperature and stirred for 1 h. Iodomethane (510 mg, 3.6 mmol, 1.2 equiv.) was added dropwise and then stirred for 3 h. The reaction mixture was quenched with water to afford a white solid. The solid was collected by filtration and dried under reduced pressure overnight. The powder was added to a flask with 2,4,6-trimethylbenzoyl chloride (1.6 g, 9.0 mmol) and *o*-dichlorobenzene (20 mL). Trifluoromethanesulfonic acid (45 mg, 0.3 mmol) was added slowly and stirred at 140 °C for 16 h. The reaction mixture was quenched with a saturated solution of sodium bicarbonate, and the aqueous layer was extracted with chloroform. The combined organic layers were stirred with sodium perchlorate for 1 h and filtered. The filtrate was concentrated *in vacuo* to afford a crude mixture. The mixture was separated by silica gel column chromatography (eluent: chloroform/methanol = 20/1 to 10/1) to a yellow crude solid. The crude solid was recrystallized with chloroform and hexane to afford 9-mesityl-2,7-dimethoxy-10-methylacridinium perchlorate as a yellow powder (112 mg, 8% yield). ^{1}H NMR (Fig. S10 in ESI†) (400 MHz, chloroform-*d*) δ 8.64 (d, *J* = 9.6 Hz, 2H), 7.95 (dd, *J* = 9.8, 3.0 Hz, 2H), 7.15 (s, 2H), 6.81 (d, *J* = 3.2 Hz, 2H), 5.06 (s, 3H), 3.78 (s, 6H), 2.48 (s, 3H), 1.76 (s, 6H). ^{13}C NMR (Fig. S11 in ESI†) (101 MHz, chloroform-*d*) δ 158.7, 155.7, 140.0, 136.5, 135.6, 131.6, 129.7, 129.2, 127.9, 120.8, 103.6, 56.0, 39.6, 21.3, 19.8. HRMS (Fig. S12 in ESI†): calcd for $C_{25}H_{26}NO_2^+$, 372.1958; found, 372.1959.

Cationic polymerization of IBVE with C1/A2 under blue LED

Cationic polymerizations using a thioester or thioacetal with an acridinium salt were carried out by a syringe technique under dry nitrogen in a flask equipped with a three-way stopcock. A typical example of the polymerization of IBVE with **C1**/**A2** under irradiation with a blue LED is given below. CH_2Cl_2 (0.86 mL), *n*-hexane (3.80 mL), *o*-dichlorobenzene (0.11 mL), IBVE (0.39 mL, 3.0 mmol), a solution of **C1** in *n*-hexane (0.60 mL, 50 mM, 0.030 mmol), and a solution of **A2** in CH_2Cl_2 (0.24 mL, 5.0 mM, 0.0030 mmol) were added into a baked 25 mL round-bottomed flask, which was equipped with a three-way stopcock and a magnetic stir bar, via dry syringes under dry nitrogen. The total volume of the reaction mixture was 6.0 mL. The flask was placed in a bath at –40 °C. The reaction was started by irradiation with a blue LED ring lamp (470 nm, 70 mW). An aliquot (0.40 mL) of the solution was removed by a syringe and quenched with triethylamine methanol. The monomer conversion was determined from the concentration of the residual monomer as measured by ^{1}H NMR with *o*-dichlorobenzene as an internal standard (93% in 80 min). The quenched reaction mixture was diluted with *n*-hexane and washed with water. The organic layer was concentrated to dryness under reduced pressure and vacuum-dried to give the polymer product (M_n = 8500, M_w/M_n = 1.24).

Measurements

^{1}H NMR spectra were recorded in $CDCl_3$ at 55 °C on a JEOL ESC-400 spectrometer operating at 400 MHz. MALDI-TOF-MS was performed on a Bruker autoflex max (linear mode) with dithranol as the ionizing matrix and sodium trifluoroacetate as the ion source. The number-average molecular weight (M_n) and molecular weight distribution (M_w/M_n) of the polymer products were determined by SEC in THF at 40 °C on two polystyrene gel columns [Shodex GPC KF-805L (8.0 mm i.d. × 30 cm) × 2; flow rate of 1.0 mL/min] connected to a JASCO PU-2080 precision pump and a JASCO RI-2031 detector. The columns were calibrated against standard polystyrene samples (Varian; M_p = 580-3242000, M_w/M_n = 1.02-1.23). Polymer samples for NMR and MALDI-TOF-MS analyses were fractionated by preparative SEC (column: Shodex K-2002) to be free from residual low-molecular-weight compounds. Photomediated polymerizations were carried out using a ring lamp with blue LEDs (CCS, LDR2-120BL2, λ_{max} = 470 nm), green LEDs (CCS, LDR2-120GR2, λ_{max} = 525 nm), or white LEDs (CCS, LDR2-120SW2, mixture) with a controller (CCS, PD3-5024-4-PI). The light intensity was measured by an optical power meter (ADCMT 8230E Optical Power Meter). Cyclic voltammetry (CV) measurements were performed with an ALS610E electrochemical analyzer in deaerated CH_2Cl_2 containing 0.1 M $Bu_4N^+ClO_4^-$ (TBAP) as a supporting electrolyte at 298 K. The platinum working electrode (BAS, surface i.d. of 1.6 mm) was polished with BAS polishing alumina suspension and rinsed with acetone before use. The counter electrode was a platinum wire (0.5 mm dia.). The measured potentials were recorded with respect to an $Ag/AgNO_3$ (0.01 M) reference electrode. The values of redox potentials (vs. $Ag/AgNO_3$) were converted into those vs. SCE by the addition of 0.29 V.[62] Fluorescence spectroscopic studies were carried out using a Horiba FluoroMax-4 spectrofluorophotometer and a Horiba Delta, type-OHK fluorescence lifetime spectrophotometer with a quartz cuvette (path length 10 mm).

Conflicts of interest

There are no conflicts of interest to declare.

Acknowledgments

This work was supported by JSPS KAKENHI Grant Numbers JP20H04809 and JP20H04819 in Hybrid Catalysis for Enabling Molecular Synthesis on Demand.

Notes and references

1 C. K. Prier, D. A. Rankic and D. W. C. MacMillan, *Chem. Rev.*, 2013, **113**, 5322–5363.
2 K. A. Margrey and D. A. Nicewicz, *Acc. Chem. Res.*, 2016, **49**, 1997–2006.
3 I. K. Sideri, E. Voutyrista and C. G. Kokotos, *Org. Biomol. Chem.*, 2018, **16**, 4596–4614.
4 Y. Lee and M. S. Kwon, *Eur. J. Org. Chem.*, 2020, 6028–6043.
5 A. Vega-Peñaloza, J. Mateos, X. Companyó, M. Escudero-Casso and L. Dell'Amico, *Angew. Chem., Int. Ed.*, 2021, **60**, 1082–1097.
6 M. V. Bobo, J. J. Kuchta III and A. K. Vannuci, *Org. Biomol. Chem.*, 2021, **19**, 4816–4834.
7 N. Corrigan, S. Shanmugam, J. Xu and C. Boyer, *Chem. Soc. Rev.*, 2016, **45**, 6165–6212.
8 M. Chen, M. Zhong and J. A. Johnson, *Chem. Rev.*, 2016, **116**, 10197–10211.
9 S. Dadashi-Silab, S. Doran and Y. Yagci, *Chem. Rev.*, 2016, **116**, 10212–10275.
10 A. M. Doerr, J. M. Burroughs, S. R. Gitter, X. Yang, A. J. Boydston and B. J. Long, *ACS Catal.*, 2020, **10**, 14457–14515.
11 M. Ciftci, G. Yilmaz and Y. Yagci, J. *Photopolym. Sci. Technol.*, 2017, **30**, 385–392.
12 M. A. Tasdelen, J. Lalevée and Y. Yagci, *Polym. Chem.*, 2020, **11**, 1111–1121.
13 B. P. Fors and C. J. Hawker, *Angew. Chem., Int. Ed.*, 2012, **51**, 8850–8853.
14 N. J. Treat, H. Sprafke, J. W. Kramer, P. G. Clark, B. E. Barton, J. R. Alaniz, B. P. Fors and C. J. Hawker, *J. Am. Chem. Soc.*, 2014, **136**, 16096–16101.
15 J. C. Theriot, C.-H. Lim, H. Yang, M. D. Ryan, C. B. Musgrave and G. M. Miyake, *Science*, 2016, **352**, 6289.
16 J. C. Theriot, B. C. McCarthy, C.-H. Lim and G. M. Miyake, *Macromol. Rapid Commun.*, 2017, **38**, 1700040.
17 D. A. Corbin, C.-H. Lim and G. M. Miyake, *Aldrichmica Acta*, 2019, **52** (1), 7–21.
18 P. S. Aklujkar and A. R. Rao, *ChemstrySelect*, 2020, **5**, 14884–14899.
19 S. de Ávila Gonçalves, P. R. Rodrigues and R. Pioli Vieira, *Macromol. Rapid Commun.*, 2012, **42**, 2100221.
20 J. Xu, K. Jung, A. Atme, A. Shanmugam and C. Boyer, *J. Am. Chem. Soc.*, 2014, **136**, 5508–5519.
21 S. Shanmugam, J. Xu and C. Boyer, *Macromol. Rapid Commun.*, 2017, **38**, 1700143.
22 J. Phommalysack-Lovan, Y. Chu, C. Boyer and J. Xu, *Chem. Commun.*, 2018, **54**, 6591–6606.

23 N. Corrigan, J. Yeow, P. Judzesitsch, J. Xu and C. Boyer, *Angew. Chem., Int. Ed.*, 2019, **58**, 5170–5189.
24 T. G. McKenzie, Q. Fu, M. Uchiyama, K. Satoh, J. Xu, C. Boyer, M. Kamigaito and G. G. Qiao, *Adv. Sci.*, 2016, **3**, 1500394.
25 M. D. Nothling, Q. Fu, A. Reyhani, A. Allison-Logan, K. Jung, J. Zhu, M. Kamigaito, C. Boyer and G. G. Qiao, *Adv. Sci.*, 2020, **7**, 2001656.
26 M. Kamigaito and M. Sawamoto, *Macromolecules*, 2020, **53**, 6749–6753.
27 M. Uchiyama, K. Satoh and M. Kamigaito, *Cationic RAFT Polymerization*, *In RAFT Polymerization*, ed. G. Moad and E. Rizzardo, Wiley-VCH, Weinheim, 2021, pp 1171−1194.
28 M .Uchiyama, K. Satoh and M. Kamigaito, *Prog. Polym. Sci.*, 2022, **124**, 101485.
29 M. Uchiyama, K. Satoh and M. Kamigaito, *Angew. Chem., Int. Ed.*, 2015, **54**, 1924–1928.
30 M. Uchiyama, K. Satoh and M. Kamigaito, *Macromolecules*, 2015, **48**, 5533–5542.
31 M. Uchiyama, K. Satoh and M. Kamigaito, *Polym. Chem.*, 2016, **7**, 1387–1396.
32 M. Uchiyama, M. Sakaguchi, K. Satoh and M. Kamigaito, *Chinese J. Polym. Sci.*, 2019, **37**, 851–857.
33 A. J. Perkowski, W. You and D. A. Nicewicz, *J. Am. Chem. Soc.*, 2015, **137**, 7580–7583
34 V. Kottisch, Q. Michaudel and B. P. Fors, *J. Am. Chem. Soc.*, 2016, **138**, 15535–15538.
35 Q. Michaudel. T. Chauviré, V. Kottisch, M. J., Supej, K. J. Stawiasz, L. Shen, W. R. Zipfel, H. D. Abruña, J. H. Freed and B. P. Fors, *J. Am. Chem. Soc.*, 2017, **139**, 15530–15538.
36 Q. Michaudel, V. Kottisch and B. P. Fors, *Angew. Chem., Int. Ed.*, 2017, **56**, 9670–9679.
37 V. Kottisch, M. J. Supej and B. P. Fors, *Angew. Chem. , Int. Ed.*, 2018, **57**, 8260–8264.
38 R. J. Sifri, A. J. Kennedy and B. P. Fors, *Polym. Chem.*, 2020, **11**, 6499–6504.
39 X. Zhang, Y. Jiang, Q. Ma, S. Hu and S. Liao S, *J. Am. Chem. Soc.*, 2021, **143**, 6357–6362.
40 S. Fukuzumi, H. Kotani, K. Ohkubo, S .Ogo, N. V. Tkachenko and H. Lemmetyinen, *J. Am. Chem. Soc.*, 2004, **126**, 1600–1601.
41 S. Fukuzumi and K. Ohkubo, *Chem. Sci.*, 2013, **4**, 561–574.
42 S. Fukuzumi, K. Ohkubo and T. Suenobu, *Acc. Chem. Res.*, 2014, **47**, 1455–1464.
43 D. A. Nicewicz and T. M. Nguyen, *ACS Catal.*, 2014, 4, 355–360.
44 A. Tlili and S. Lakhdar, *Angew. Chem., Int. Ed.*, 2021, **60**, 19526–19549.
45 H.-J. Timpe, S. Ulrich, C. Decker and J.-P. Fouassier, *Eur. Polym. J.*, 1994, **30**, 1301–1307.
46 K. A. Ogawa, A. E. Goetz and A. J. Boydston, *J. Am. Chem. Soc.*, 2015, **137**, 1400–1403.
47 W. D. Cook, S. Chen, F. Chen, M. U. Kahveci and Y. Yagci, *J. Polym. Sci.: Part A: Polym. Chem.*, 2009, **47**, 5474–5487.
48 S. Chen, W. D. Cook and F. Chen, *Macromolecules*, 2009, **42**, 5965–5975.
49 B. L. Buss, C.-H. Lim and G. M. Miyake, *Angew. Chem., Int. Ed.*, 2020, **59**, 3209–3217.
50 Y. Liu, Q. Chen, Y. Tong and Y. Ma, *Macromolecules*, 2020, **53**, 7053–7062.
51 The cationic polymerization of IBVE with **C1**/**A1** was also conducted at 0 °C under blue LED irradiation in CH_2Cl_2 ($[M]_0/[\mathbf{C1}]_0/[\mathbf{A1}]_0$ = 500/2.5/0.50 mM). However, the reaction was slower (99% conversion in 7 h) than at –40 °C (98% conversion in 80 min) under the same conditions to result in polymers with lower M_n values than the calculated ones (M_n(calcd) = 20300 vs M_n(obsd) = 9000) (M_w/M_n = 1.69).
52 One-electron reduction potentials were determined by the cyclic voltammetric measurements (see Fig. S2 in ESI†). The procedure is shown in the experimental section. The potentials at the excited state were determined by adding the excited energy (2.72 eV).[40]
53 K. Ohkubo, K. Mizushima, R. Iwata, K. Souma, N. Suzuki and S. Fukuzumi, 2010, **46**, 601–603.
54 The quantum yield of electron transfer state of **A6** was determined from the fluorescence lifetime (18.5 ns) and the non-mesitylene substituted acridinium salt (37 ns).[42]
55 M. Konya, M. Uchiyama, K. Satoh and M. Kamigaito, *ChemPhotoChem*, 2019, **3**, 1100–1108.T. Tsudaka, H. Kotani, K. Ohkubo, T. Nakagawa, N. V. Tkachenko, H. Lemmetyinen and S. Fukuzumi, *Chem.-Eur. J.*, 2017, **23**, 1306–1317.
56 S. Fukuzumi, K. Ohkubo, T. Suenobu, K. Kato, M. Fujitsuka and O. Ito, *J. Am. Chem. Soc.*, 2001, **123**, 8459–8467.
57 The polymerization with **C1**/**A2** under blue LED irradiation at 0 and 20 °C in *n*-hexane/CH_2Cl_2 = 4/1 ($[M]_0/[\mathbf{C1}]_0/[\mathbf{A2}]_0$ = 500/5.0/ 0.20 mM) did not produce any polymers.
58 L. Wang, F. Wu, J. Chen, D. A. Nicewicz and Y. Huang, *Angew. Chem., Int. Ed.*, 2017, **56**, 6896–6900.
59 H. Aoshima, M. Uchiyama, K. Satoh and M. Kamigaito, *Angew. Chem., Int. Ed.*, 2014, **53**, 10932–10936.
60 S. Kumagai, K. Nagai, K. Satoh and M. Kamigaito, *Macromolecules*, 2010, **43**, 7523–7531.
61 C. K. Mann and K. K. Barnes, *Electrochemical Reactions in Non-aqueous Systems*, Mercel Dekker, New York, 1970.

